IDA

INSTITUTE FOR DEFENSE ANALYSES

Contagious Disease Dynamics for Biological Warfare and Bioterrorism Casualty Assessments

John N. Bombardt, Jr.

February 2000

Approved for public release; distribution unlimited.

IDA Paper P-3488

Log: H 00-000561

20010221 089

This work was conducted under contract DASW01 98 C 0067, Task DM-6-1845, for the Joint Program Office for Biological Defense. The publication of this IDA document does not indicate endorsement by the Department of Defense, nor should the contents be construed as reflecting the official position of that Agency.

© 2000, 2001 Institute for Defense Analyses, 1801 N. Beauregard Street, Alexandria, Virginia 22311-1772 • (703) 845-2000.

This material may be reproduced by or for the U.S. Government pursuant to the copyright license under the clause at DFARS 252.227-7013 (NOV 95).

INSTITUTE FOR DEFENSE ANALYSES

IDA Paper P-3488

Contagious Disease Dynamics for Biological Warfare and Bioterrorism Casualty Assessments

John N. Bombardt, Jr.

PREFACE

This document was prepared by the Institute for Defense Analyses in partial fulfillment of the task order "Planning Guide for Estimation of NBC Battle Casualties, Volume 2: Biological," sponsored by the Joint Program Office for Biological Defense and the U.S. Army Surgeon General.

The author would like to thank Dr. Jeffrey Grotte, Dr. Nathan Platt and Ms. Julia Klare Burr of the Institute for Defense Analyses. Their comments and suggestions regarding this publication were most helpful, but any remaining shortcomings are those of the author.

CONTENTS

I. INTRODUCTION AND SUMMARY 1

II. THE SEIR FRAMEWORK AND AN EHF EPIDEMIC 5

A. Haydon-Woolhouse-Kitching SEIR Algorithm 5

B. EHF Epidemiological Data 7

III. AVERAGE NEW INFECTIONS PER UNIT TIME 10

A. Characterization of the Random Variables 11

B. Monte Carlo Results 13

C. Average Daily New Infections in a Format for SEIR Calculations 16

IV. SEIR RESULTS 17

A. Retrospective Investigation 17

B. Predictions for Equivalent Epidemiological Circumstances 22

C. Unique Epidemiological Circumstances and Their Impact 27

V. CONCLUDING OBSERVATIONS 32

FIGURES

II-1. Ebola Hemorrhagic Fever Fatalities in the Bandundu Region of the Democratic Republic of the Congo from 2 March through 16 July 1995 9

II-2. Onset of Ebola Hemorrhagic Fever Symptoms During the 1995 Outbreak in the Democratic Republic of the Congo 9

III-1. Normal and Weibull Probability Density Functions (PDFs) for the Random Variable σ (Incubation Period) 12

III-2. Normal and Lognormal Probability Density Functions (PDFs) for the Random Variable ζ (Infection-to-Removal Period) 12

III-3. Average Daily Exposures (Average New Infections Per Unit Time) for the Two Epidemiological Data Sets of Figures II-1 and II-2, Normally Distributed Random Variables, and 1000 Monte Carlo Trials 14

III-4. Average Daily Exposures (Average New Infections Per Unit Time) for the Two Epidemiological Data Sets of Figures II-1 and II-2, Weibull and Lognormal Distributions, and 1000 Monte Carlo Trials 14

III-5. Average Fatal (Red or Dark) and Nonfatal (White) Daily Exposures for the Two Epidemiological Data Sets of Figures II-1 and II-2, Normally Distributed Random Variables, and 1000 Monte Carlo Trials 15

III-6. Average Fatal (Red or Dark) and Nonfatal (White) Daily Exposures for the Two Epidemiological Data Sets of Figures II-1 and II-2, Weibull and Lognormal Distributions, and 1000 Monte Carlo Trials 16

III-7. Censored Version of Average Fatal and Nonfatal Daily Exposures in Figure III-5 17

IV-1. Time-Varying Total Number of Removed Individuals that Is Calculated from the Average Daily Exposures in Figure III-7 19

IV-2. Instantaneous Numbers of Exposed (Incubating) and Infectious Individuals that Are Calculated from the Average Daily Exposures in Figure III-7 20

IV-3. Calculated Time-Varying Rate of Disease Transmission, β, for the 1995 EHF Outbreak in Kikwit, DRC. The Solid (or Dashed) Curve Represents the Disease Transmission Rate for a Total Exposable Population of 200,000 (or 1,000) 21

IV-4. Instantaneous Number of Individuals in the Exposed Cohort for Different Initial Conditions (1, 5, 10, 15, and 20 Exposures on Day 0) and a Total Exposable Population of 200,000 23

IV-5. Instantaneous Number of Individuals in the Infectious Cohort for Different Initial Conditions (1, 5, 10, 15, and 20 Exposures on Day 0) and a Total Exposable Population of 200,000 24

IV-6. Cumulative Number of Individuals in the Removed Cohort for Different Initial Conditions (1, 5, 10, 15, and 20 Exposures on Day 0) and a Total Exposable Population of 200,000 24

IV-7. Instantaneous Number of Individuals in the Exposed Cohort for Different Initial Conditions (1, 5, 10, 15, and 20 Exposures on Day 0) and a Total Exposable Population of 1,000 25

IV-8. Instantaneous Number of Individuals in the Infectious Cohort for Different Initial Conditions (1, 5, 10, 15, and 20 Exposures on Day 0) and a Total Exposable Population of 1,000 26

IV-9. Cumulative Number of Individuals in the Removed Cohort for Different Initial Conditions (1, 5, 10, 15, and 20 Exposures on Day 0) and a Total Exposable Population of 1,000 26

IV-10. Total Number of Removals as a Function of the Number of Initial Infections for Exposable Populations of 200,000 and 1,000 27

IV-11. Instantaneous Number of Individuals in the Exposed Cohort for 1,000 Initial Infections and for Various Total Populations 29

IV-12. Instantaneous Number of Individuals in the Infectious Cohort for 1,000 Initial Infections and for Various Total Populations 29

IV-13. Cumulative Number of Individuals in the Removed Cohort for 1,000 Initial Infections and for Various Total Populations 30

IV-14. Total Number of Removals versus the Total Population for 1,000 Initial Infections 30

IV-15. Instantaneous Projected Number of Removals for 1,000 Initial Infections and for Various Total Populations 31

I. INTRODUCTION AND SUMMARY

As recently as 1991, the Former Soviet Union (FSU) reportedly stockpiled weapons with bacterial and viral payloads that cause anthrax, pneumonic plague, glanders, smallpox, Marburg hemorrhagic fever and other diseases.[1] The end of the Cold War and the 1992 Russian ban on all biological weapon activity, however, lend credence to Russian claims regarding the complete destruction of FSU biological weapon stockpiles. Unfortunately, the immensity of the FSU biological warfare (BW) program and the corresponding potential for international proliferation of BW capabilities remain troubling realities.[2]

Upwards of eight countries may now have, or may be pursuing, biological weapons of mass destruction (WMD).[3] Iraq's relentless pursuit of biological weapons during the 1980s and 1990s[4] is a clear signal that future adversaries of the U.S. may also be willing to bear great costs and risks in acquiring and maintaining BW capabilities. Moreover, since biological weapons are probably already in arsenals of totalitarian regimes, the U.S. is forced to deal with both BW and state-sponsored bioterrorism threats. Domestic bioterrorism issues are also receiving considerable attention at various levels of government.

Preventing, treating, and managing mass casualties are key activities of military and civilian health care providers in response to either offensive BW operations or bioterrorist attacks.[5,6] These medical countermeasures will be most effective when the disseminated disease-causing agents and the initially exposed people are rapidly identified. If neither the biological agents nor the exposed individuals are known, there may be no opportunities for preventative or prophylactic measures; health care providers

---

[1] 1998 Congressional Hearings on Intelligence and Security, Joint Economic Committee of the United States Congress, *Terrorist and Intelligence Operations: Potential Impact on the U.S. Economy,* Statement by Dr. Kenneth Alibek, May 20, 1998.

[2] Office of the Secretary of Defense, *Proliferation: Threat and Response*, November 1997, p. 46. Concerns about proliferation span the spectrum from sharing biological warfare expertise through selling biological weapon hardware.

[3] *Proliferation: Threat and Response*, pp. 5, 9, 16, 25, 30, 34, 38, and 42.

[4] 1998 Counterproliferation Program Review Committee Report to Congress, *Report on Activities and Programs for Countering Proliferation and NBC Terrorism,* Figure 3.2, pp. 3-12.

[5] U.S. Army Medical Research Institute of Infectious Diseases, *Medical Management of Biological Casualties*, Handbook, Third Edition, July 1998.

[6] Arnold F. Kaufmann, Martin I. Meltzer, and George P. Schmid, *The Economic Impact of a Bioterrorist Attack: Are Prevention and Postattack Intervention Programs Justifiable?*, Emerging Infectious Diseases, Vol. 3, No.2, April-June 1997.

must then "catch up" with the disease as it unfolds. This latter course of action is perilous, especially in the case of a highly contagious disease like smallpox. By the time a symptomatic individual seeks medical attention and the contagious disease is accurately diagnosed, he or she might have already infected many other individuals and an epidemic could be well under way.[7]

A weapon or terrorist device containing the causal agent of a contagious and incurable disease represents a double-edged sword. The primary offensive advantage is that just one initial infection could lead to tens or even hundreds of casualties, including a significant number of health care providers. On the other hand, the main disadvantage of such a weapon or device is the risk that it might backfire on the attacker or may even initiate a pandemic with widespread, unintended consequences. This disadvantage is undoubtedly one reason why FSU biological weapon doctrine emphasized the following effect-target pairs: a) lethal diseases and long-range strategic targets at great distances from the FSU, and b) incapacitating diseases and medium-range theater targets well beyond the front lines.[8]

The present study describes an approach for quantitatively analyzing the spread of a contagious disease that could be initiated by either the military employment of a biological weapon or an act of bioterrorism. Of particular interest here are time histories of four cohorts: 1) Susceptible individuals, 2) Exposed and infected (incubating) individuals, 3) Infectious (contagious) individuals, and 4) Removed (alive and noncontagious, or dead) individuals. The objective SEIR curves characterize health care and mortuary service needs as functions of time for a known disease, for given initial conditions, and for an assumed time-varying rate of disease transmission.

Disease characteristics such as mean values and standard deviations of both the incubation period and the period from infection until removal comprise the input for the SEIR approach under consideration. Beginning numbers of individuals for all four cohorts are the initial conditions that must also be specified as input. Perhaps most importantly, the present approach calls for a time-varying rate of disease transmission to be derived from actual epidemic data.

Within the SEIR framework, new and "successful" exposures entail both an increase in the size of the exposed cohort and an offsetting decrease in the size of the

---

[7] Potomac Institute for Policy Studies, *Seminar on Emerging Threats of Biological Terrorism: Recent Developments*, Proceedings Report, PIPS-98-3, 16 June 1998, p. 16.

[8] *Terrorist and Intelligence Operations: Potential Impact on the U.S. Economy.*

susceptible cohort. Newly exposed and infected individuals stay in the exposed cohort throughout the average incubation period, after which they immediately enter the infectious cohort. During their dwell time in the infectious cohort, symptomatic individuals expose and infect susceptible individuals in accordance with epidemiological circumstances and disease characteristics. The SEIR sequence finally comes to an end for an individual when he or she leaves the infectious cohort and enters the removed cohort, wherein each member is either alive and immune, or dead and no longer a source of infection.

Certain epidemiological circumstances surround any outbreak of a disease and these (along with disease characteristics) virtually determine the rate at which the disease is transmitted from person to person. These circumstances encompass factors such as physical profiles of the susceptible cohort, frequency and types of possible contacts between infectious and susceptible individuals, prevailing health care practices, health care system capacity, and disease awareness levels. To be sure, the epidemiological circumstances surrounding a recorded outbreak are unlikely to be fully reproduced in any future outbreak, but an assumption of similarity provides a logical basis for predictions of BW or bioterrorism casualties.

Epidemic models come in many shapes and sizes: empirical, semi-empirical, linear, nonlinear, deterministic, stochastic, spatial, temporal, continuous, discrete, et cetera.[9] This paper adapts and extends a nonlinear, deterministic, discrete-time model that was developed for analyses of measles in human populations, as well as foot and mouth disease among cattle herds.[10] This SEIR algorithm with a time-varying disease transmission rate is a flexible and powerful tool for understanding disease dynamics, especially when disease characteristics and the driving source function can be derived from observations. It is the dynamics of a contagious disease, as opposed to its spatial or geographical distribution, that receives attention herein.

The number of new infections per unit time drives the aforementioned SEIR model. In general, dates of new infections in an actual epidemic are not observable in the same sense as dates of death, or even symptom onset dates. The former dates usually must be inferred from the latter ones. But the date of a new infection is related to a date

---

[9] Denis Mollison (Ed.), *Epidemic Models: Their Structure and Relation to Data* (Cambridge University Press, Publications of the Newton Institute, 1995), pp. 17-33. Part I of this book puts forward a conceptual framework for epidemic models and describes several fundamental methodological issues.

[10] D. T. Haydon, M. E. J. Woolhouse, and R. P. Kitching, *An analysis of foot-and-mouth-disease epidemics in the UK*, IMA Journal of Mathematics Applied in Medicine & Biology, Vol. 14, 1997, pp. 1-9.

of death or to a symptom onset date through a random variable: respectively, the period from the new infection until death, or just the period of incubation. One way of inferring new infection dates is simply to use an average value of the appropriate random variable, and this path was followed by Haydon, Woolhouse, and Kitching. In the present study, average new infections per unit time are derived from epidemiological data by applying the Monte Carlo method.[11]

Comprehensive epidemiological information is now available on the 1994-1996 African outbreaks of Ebola hemorrhagic fever (EHF).[12] In particular, the 1995 EHF outbreak in Kikwit, Democratic Republic of the Congo,[13] began with one initial infection (the "index" case) and ultimately involved 315 cases, including 255 fatalities. Two series of epidemiological data for this Kikwit EHF outbreak are excellent vehicles to demonstrate the potential of a semi-empirical approach. The Monte Carlo method is thus applied to daily fatality data and to daily symptom onset data. Next, two differing sets of Monte Carlo calculations are reconciled and, as a consequence, the results for average new infections per unit time reflect both deaths and recoveries. These daily infection results are, in turn, used with the Haydon-Woolhouse-Kitching SEIR algorithm to evaluate cohort time histories and the time-varying rate of disease transmission.[14]

With a semi-empirical time-varying rate of disease transmission in hand, the Haydon-Woolhouse-Kitching algorithm can be revisited to address "what-if" questions. For instance, if a future offensive BW operation or bioterrorist attack infected ten people with the Ebola virus, and if these ten infections were surrounded by epidemiological circumstances like those of the 1995 EHF outbreak in Kikwit, what would happen? How many people would be infected as a function of time? How many people would become ill as a function of time? What would be the total number of fatalities?

In essence, a key analytical objective of the present study is to forge new and meaningful links between deterministic "mean-field" epidemic models and inherently random outbreak data (symptom onset dates, for example, or dates of death). Another important analytical objective is to explore the predictive value of these links.

---

[11] Ilya M. Sobol', *A Primer for the Monte Carlo Method* (CRC Press, Inc., 1994), pp. 40-47.

[12] See the special 300-page supplement (Volume 179, Supplement 1) to the Journal of Infectious Diseases (JID) for February 1999.

[13] Ali S. Khan, F. Kweteminga Tshioko, David L. Heymann et al, *The Reemergence of Ebola Hemorrhagic Fever, Democratic Republic of the Congo, 1995*, JID, Vol. 179 (Supplement 1), pp. S76-S86.

[14] Epidemiological circumstances surrounding the 1995 EHF outbreak in Kikwit are characterized or represented by this semi-empirical time-varying rate of disease transmission. These circumstances are described in the preceding reference and they are reviewed in the main body of this paper.

The main body of this paper covers the analytical framework and input, a requisite transitional investigation, and output. With regard to framework and input, the author examines the SEIR algorithm and reviews epidemiological aspects of the Kikwit EHF outbreak. The next items for discussion are Monte Carlo calculations and the derivation of average new infections per unit time. In terms of output, there are both retrospective and predictive SEIR results. And finally, observations on principal findings and unresolved issues are presented.

II. THE SEIR FRAMEWORK AND AN EHF EPIDEMIC

A. Haydon-Woolhouse-Kitching SEIR Algorithm

In analyzing the dynamics of foot and mouth disease among cattle herds in the United Kingdom, the investigators (Haydon, Woolhouse, and Kitching) introduced a set of four finite-difference equations.[15] These equations relate the susceptible (S), exposed (E), infectious (I), and removed (R) cohorts and they also determine time dependencies through a time-varying disease transmission rate (ξ). For a single time step Δt and an arbitrary number n of time steps, the equations can be written as follows:

(1) $S[n] = S[n-1] - P[n-1] \times \Delta t,$

(2) $E[n] = E[n-1] + (P[n-1] - P[n-\sigma_a - 1]) \times \Delta t,$

(3) $I[n] = I[n-1] + (P[n-\sigma_a - 1] - P[n-\zeta_a - 1]) \times \Delta t,$

(4) $R[n] = R[n-1] + P[n-\zeta_a - 1] \times \Delta t$

and

(5) $P[n] = \xi[n] \times S[n] \times I[n].$

Equations (2), (3), and (4) contain the parameters σ_a and ζ_a which are, respectively, the average dwell time in the exposed cohort (or average incubation period) and the average dwell time in both exposed and infectious cohorts (or average period from infection to removal).[16] In addition, this algorithm also invokes the assumption of a time-independent total population, N_0:

(6) $N_0 = S[n] + E[n] + I[n] + R[n].$

[15] *An analysis of foot-and-mouth-disease epidemics in the UK*, p.4.

[16] Haydon, Woolhouse, and Kitching chose to use the sum of σ_a and v_a instead of ζ_a, where v_a is the average dwell time in the infectious cohort. These quantities must be expressed as integral multiples of the time step to implement the algorithm.

The function P connects the SEIR cohorts and it deserves special attention. Generally speaking, since P represents a nonlinearity, the algorithm's results for one set of initial conditions cannot be scaled in a linear fashion to obtain valid results for other initial conditions. Moreover, there are three distinct interpretations of the function P. A close look at equations (1) and (2) reveals that $P[n-1]\times\Delta t$ is the number of new infections at time step n (or, in other words, the number of individuals that leave the susceptible cohort and enter the exposed cohort at time step n). And similarly, $P[n-\sigma_a -1]\times\Delta t$ is the number of individuals that leave the exposed cohort and enter the infectious cohort at time step n, while $P[n-\zeta_a -1]\times\Delta t$ is the number of individuals that leave the infectious cohort and enter the removed cohort at time step n.[17]

Connections between the function P and the four cohorts suggest the types of epidemiological information that could be employed to implement the algorithm. Dates of entry for the removed cohort comprise the epidemiological data that are most likely to be available. Occasionally, entry dates for the infectious cohort (or, more accurately, symptom onset dates) are reportable characteristics of an outbreak or epidemic. But new infection dates (i.e., entry dates for the exposed cohort) tend to be either unknown or very uncertain epidemiological data.

By analogy with chemical reaction kinetics[18], mathematical epidemiologists often assume that contacts between susceptible and infectious individuals are random and that the possible number of such contacts is proportional to the product of S and I. This assumption, the previous observation concerning $P[n-1]\times\Delta t$, and equation (5) lead to the interpretation that $\xi[n-1]\times\Delta t$ is the fraction of all possible contacts between susceptible and infectious individuals at time step n-1 that becomes infected at time step n. In the same vein, when $P[n-1]\times\Delta t$ is divided by $I[n-1]$, this ratio becomes the number of new infections at time step n per infectious individual at time step n-1.

Haydon, Woolhouse, and Kitching acquired data on the destruction of diseased cattle herds and constructed an empirical time history of the removed cohort. To

[17] An individual in the context of this SEIR algorithm is an epidemiological unit, which could be one person, one animal, one plant or even a collection thereof. In the paper by Haydon, Woolhouse, and Kitching, the epidemiological unit is the herd of cattle on a single farm.

[18] *Epidemic Models: Their Structure and Relation to Data*, p. 85. Contacts between individuals are likened to molecular collisions, but the contacts of interest may be either direct or indirect. Interesting contacts can involve the transfer of contagia from infectious to susceptible individuals, and transfer mechanisms include intimate physical interactions, handling of biohazardous materials, handshakes, face-to-face conversations and droplet projections, inhalation of an infectious aerosol, etc.

implement their algorithm, they took four separate steps: a) estimate the average incubation and infectious periods; b) derive P from equation (4); c) solve equations (1), (2), and (3) to determine the other cohort time histories; and d) obtain the time-varying rate of disease transmission from equation (2). This retrospective analysis provided new information on the temporal nature of a virulent epidemic, roles of primary and secondary infections, and the effectiveness of disease control measures.

A self-consistency problem arises, however, when the algorithm is implemented in the above manner. More specifically, because the foregoing implementation involves the direct utilization of raw epidemiological data (which reflect various incubation and infectious periods), the algorithm's input is inconsistent with its output (which can only describe the average progression of an epidemic). This input-output inconsistency will occur whenever actual or observed removal times are uniformly shifted by ζ_a time steps to define the new infection rate.[19]

To achieve a self-consistent implementation of the algorithm, an average time history for the new infection rate must be extracted from both epidemiological data and realistic variations in either infection-to-removal times or symptom onset times, as appropriate. A transitional investigation is thus necessary to connect epidemiological data and its inherent randomness with a deterministic epidemic model. This matter will be carefully addressed after a discussion of the 1995 EHF outbreak in equatorial Africa.

B. EHF Epidemiological Data

The 1995 EHF outbreak in the Bandundu region of the Democratic Republic of the Congo (DRC) extended from early January until the 16th of July.[20] Both of the major health care facilities in this southern DRC region, the Kikwit II Maternity and Kikwit General Hospitals, were engulfed by EHF patients, and 80 health care workers succumbed to the disease. By the beginning of May 1995, more than 50 southern DRC residents had died of EHF. Even though the very first EHF outbreak took place in the northern DRC and it claimed 280 lives in 1976, not until early May did southern DRC health officials come to believe that EHF (rather than epidemic dysentery) was again the cause of numerous deaths.

---

[19] The same inconsistency would occur if observed symptom onset times were uniformly shifted by σ_a time steps to arrive at P[n-1].

[20] Descriptive information on this EHF outbreak in the DRC is from *The Reemergence of Ebola Hemorrhagic Fever, Democratic Republic of the Congo, 1995.* The outbreak happened in and around the city of Kikwit, which then encompassed a population of about 200,000.

The Centers for Disease Control (CDC) in the U.S. received specimens on the 9th of May; subsequent test results showed that the Ebola virus (Zaire subtype) was indeed the causative agent for the disease in 14 patients. An international commission was quickly established for the management of this EHF outbreak. The commission's activities encompassed, among other things, training sessions for numerous health care workers and physicians on the 12th and 14th of May, as well as the provision of protective clothing and equipment.

EHF signs and symptoms are diverse. Initially, the infected individual may experience an abrupt onset of fever, a severe frontal headache, malaise, loss of appetite, joint and diffuse muscle pain, loss of strength, and perhaps a slow heartbeat or conjunctival inflammation. Intermediate symptoms might be non-bloody or bloody diarrhea, abdominal pain, pharyngitis, difficulty in breathing, severe nausea, and vomiting. In the final stage of the disease, there could be a maculopapular rash and uncontrolled bleeding, and the afflicted individual may then go into shock and die.

Case records for 310 diseased individuals showed that 53 percent were female, the median age was 37 years (with a range from two months to 71 years), and the average age of survivors (~32.8 years) was about five years younger than that of nonsurvivors (~38.5 years). A review of 224 case records also yielded a mean period of 9.6 days from symptom onset to death.

Reliable dates of death for 237 EHF cases and approximate dates of symptom onset for 291 EHF cases are displayed in Figures II-1 and II-2, respectively. The first date of death in Figure II-1 is the 2nd of March; the first date of EHF symptom onset in Figure II-2 is the 6th of March. Missing, incomplete, and inaccurate case records prevented researchers from constructing complete sets of epidemiological data; in other words, Figure II-1 does not account for all 255 EHF deaths and Figure II-2 doesn't encompass all 315 EHF cases. Another void occurs because published accounts of the Kikwit EHF outbreak do not identify corresponding dates of symptom onset and death.

The 1976 EHF outbreak in the DRC lasted about two months and involved extensive nosocomial transmission of the disease (i.e., transmission taking place in a hospital) primarily because needles and syringes were reused without sterilization. Eighteen years later, the second EHF outbreak in the DRC lasted six months and involved several waves of nosocomial transmission, albeit there was little or no reuse of unsterile needles or syringes. Epidemiological findings (new symptomatic cases after the 12th of May or after day 90 in Figure II-2) suggest that the 1995 outbreak was finally

brought under control when health care providers adhered to strict barrier nursing procedures and when they routinely utilized protective clothing and equipment.

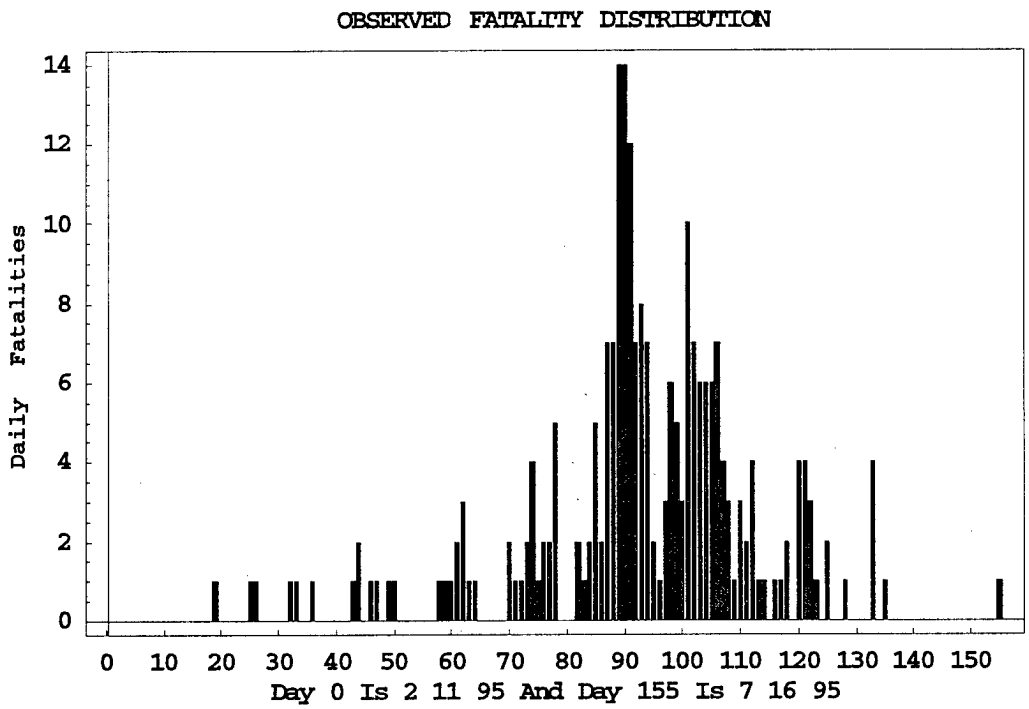

Figure II-1. Ebola Hemorrhagic Fever Fatalities in the Bandundu Region of the Democratic Republic of the Congo from 2 March through 16 July 1995.

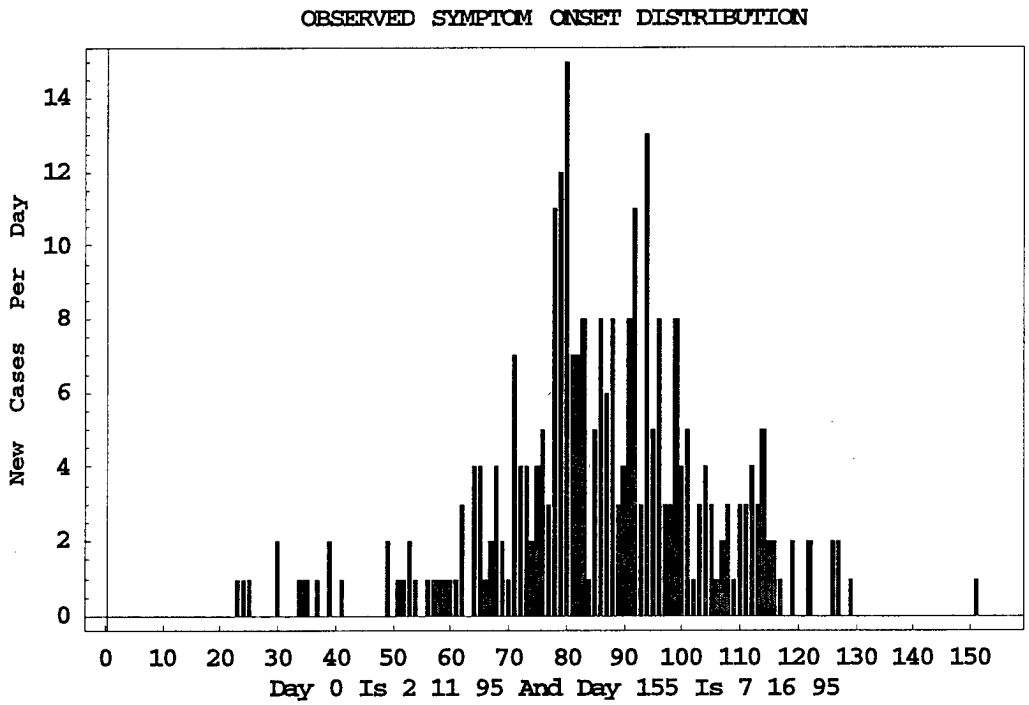

Figure II-2. Onset of Ebola Hemorrhagic Fever Symptoms During the 1995 Outbreak in the Democratic Republic of the Congo.

Epidemiological evidence from the 1995 outbreak strongly indicates that the disease was transmitted to susceptible individuals through direct person-to-person contacts, the projection of infectious droplets directly onto mucous membranes, and other contacts with infectious body fluids. This evidence also indicates that the disease is rarely transmitted from one person to another via an infectious aerosol, especially at distances of a few meters or more. Lastly, burial rituals and direct contacts with cadavers may have infected some susceptible individuals.

The international public health community was surprised by the 1995 EHF outbreak in Kikwit.[21] This community now recognizes that disease-detection capabilities, disease-response systems, and basic public health practices must all be improved in developing countries. Additionally, it recognizes the need for better international preparedness and the importance of accessible protective equipment and supplies.

III. AVERAGE NEW INFECTIONS PER UNIT TIME

The basic problem at hand is to backtrack from fatality or symptom onset observations and to derive average new infections per unit time. At the core of this problem are random variations of the infection-to-removal time and the incubation period. One convenient way to numerically simulate random variables is the Monte Carlo method, and a straightforward computerized application of the method generates a temporal profile of new infections for each statistical trial. Furthermore, numerous Monte Carlo trials yield a statistical database, which is amenable to analysis using the standard tools of descriptive statistics.

There are four principal steps in the computable algorithm for a single Monte Carlo trial. First, randomly select and then round off an infection-to-removal time (or incubation period) for each and every fatality (or case of symptom onset). Second, backtrack in time to identify when all infections occurred. Third, compile the total score for each time step. And fourth, save the calculated temporal profile of new infections for subsequent manipulation. In the case of the 1995 EHF outbreak in Kikwit, two sets of complementary epidemiological data are available (Figures II-1 and II-2); consequently, the four-step algorithm must be executed twice.

---

[21] David L. Heymann, Deo Barakamfitiye, Mark Szczeniowski et al, *Ebola Hemorrhagic Fever: Lessons from Kikwit, Democratic Republic of the Congo*, JID, Vol. 179 (Supplement 1), pp. S283-S286.

Monte Carlo trials for symptom onset data and a separate database of trials for fatality data are resources for the construction of three average temporal profiles of new infections. One average temporal profile (from symptom onset data) encompasses survivors and nonsurvivors, another average profile (from fatality data) deals only with nonsurvivors, and the corresponding difference profile characterizes new infections just among survivors. Because dates of death usually are more reliable than symptom onset dates, there is a reconciliation of average new infections per unit time for nonsurvivors with average new infections per unit time just for survivors, and it produces a composite temporal distribution of all new infections.

All computations for this paper were performed on a personal computer using Mathematica software.[22] Mathematica notebooks with numerical procedures and results are obtainable from the author.

A. Characterization of the Random Variables

The incubation period for EHF depends on how the individual is infected with the Ebola virus. A needle stick or other mishap during a surgical procedure on an infectious patient could infect a health care professional who, in turn, would exhibit symptoms in two or three days. Less direct modes of infection may produce symptoms in several days or even a few weeks. A mean incubation period of nine days and a standard deviation of two days are assumed for the 1995 EHF outbreak in Kikwit.

As indicated previously, fatality and symptom onset data from the Kikwit outbreak show that the mean time from symptom onset until death was about 10 (or, more precisely, 9.6) days. The mean infection-to-removal time is therefore estimated to be 19 days, with an assumed standard deviation of three days.

The incubation period, σ, and the infection-to-removal time, ζ, are random variables without well-defined probability distributions. To examine influences of different distributional assumptions, the joint probability distribution of σ and ζ is defined to be either the product of independent normal distributions or the product of independent Weibull and lognormal distributions.[23] Normal distributions are selected because of their prevalence, but Weibull and lognormal distributions are often employed in reliability and

[22] Stephen Wolfram, *The Mathematica Book*, 3rd ed., (Wolfram Media/Cambridge University Press, 1996).

[23] Lennart Rade and Bertil Westergren, *BETA Mathematics Handbook*, 2nd ed., (CRC Press, 1990), pp. 375 and 395.

hazard models.[24] Plots of the alternative distributions for the two random variables appear in Figures III-1 and III-2.

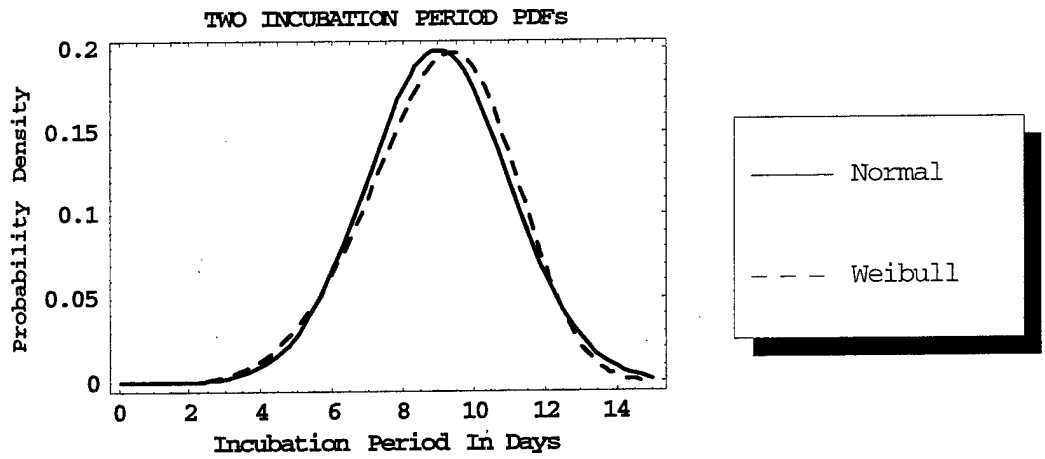

Figure III-1. Normal and Weibull Probability Density Functions (PDFs) for the Random Variable σ (Incubation Period).

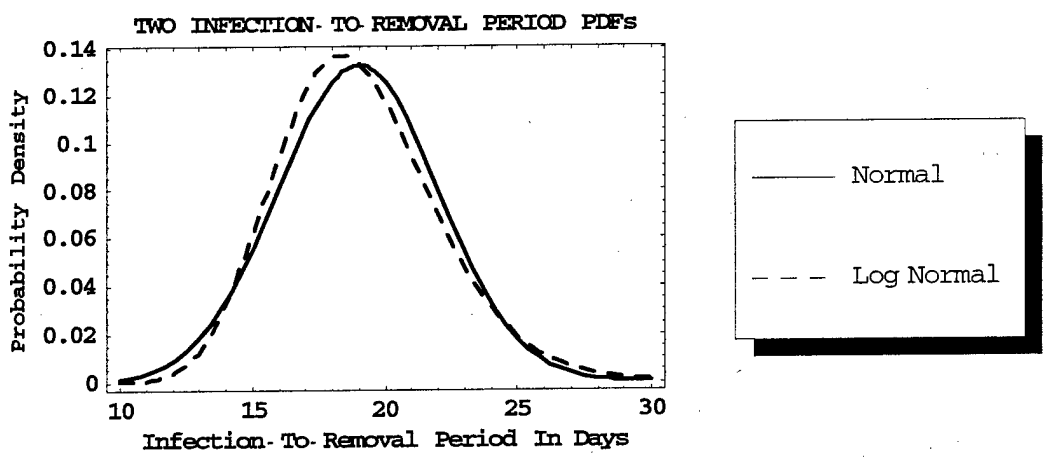

Figure III-2. Normal and Lognormal Probability Density Functions (PDFs) for the Random Variable ζ (Infection-to-Removal Period).

[24] Paul A. Tobias and David C. Trindade, *Applied Reliability* (Van Nostrand Reinhold Company, 1986). The Weibull distribution tends to be most applicable when the first of many flaws (immune system limitations) produces a failure (symptom onset), whereas the lognormal distribution is often applicable when a degradation process (illness) leads to a failure (death).

B. Monte Carlo Results

The epidemiological data sets in Figures II-1 and II-2, along with the PDFs in Figures III-1 and III-2, constitute the input for Monte Carlo calculations. In accordance with the previous description of the four-step algorithm, the computer completes a Monte Carlo trial when the number of new infections at every time step is determined for each set of input data. One time series of observations and a total of K Monte Carlo trials clearly yield a sample of K separate values for the number of new infections at each time step, and a sample mean differs from the true mean by some amount ε. Defining Σ as the true standard deviation about the true mean, a "loose" bound[25] on the error in a sample mean is

$$(7) \quad \varepsilon < 3\Sigma/\sqrt{K}.$$

For 1,000 Monte Carlo trials and a true standard deviation of either 2 or 3, equation (7) tells us that the error in a sample mean would be less than 0.19 or 0.28, respectively. In practice, such error bounds tend to be of less concern than probable errors, which are smaller by a factor of 4.45.[26]

Figure III-3 displays two profiles of average daily exposures (i.e., average new infections per unit time) for normally distributed random variables; similarly, Figure III-4 shows comparable profiles for the Weibull and lognormal distributions. One common temporal profile in these two figures is associated with an input of fatality data; the other common profile is related to an input of symptom onset data. Though qualitative differences between like profiles in Figures III-3 and III-4 tend to be insignificant, a few quantitative differences between unlike profiles in the same figure suggest some incompatibilities between the two sets of epidemiological data. Specifically, with regard to the time frame from day 70 to day 76 in both figures, symptom-related and fatality-related average daily exposures can differ by substantial negative amounts.

If the set of fatality data in Figure II-1 is indeed relatively reliable, the above-mentioned negative differences between average numbers of daily exposures would point to inaccuracies in the symptom onset data (Figure II-2). To better understand quantitative differences that matter most, other graphical comparisons are necessary.

---

[25] *A Primer for the Monte Carlo Method*, pp. 15-16.

[26] *A Primer for the Monte Carlo Method, p.16.*

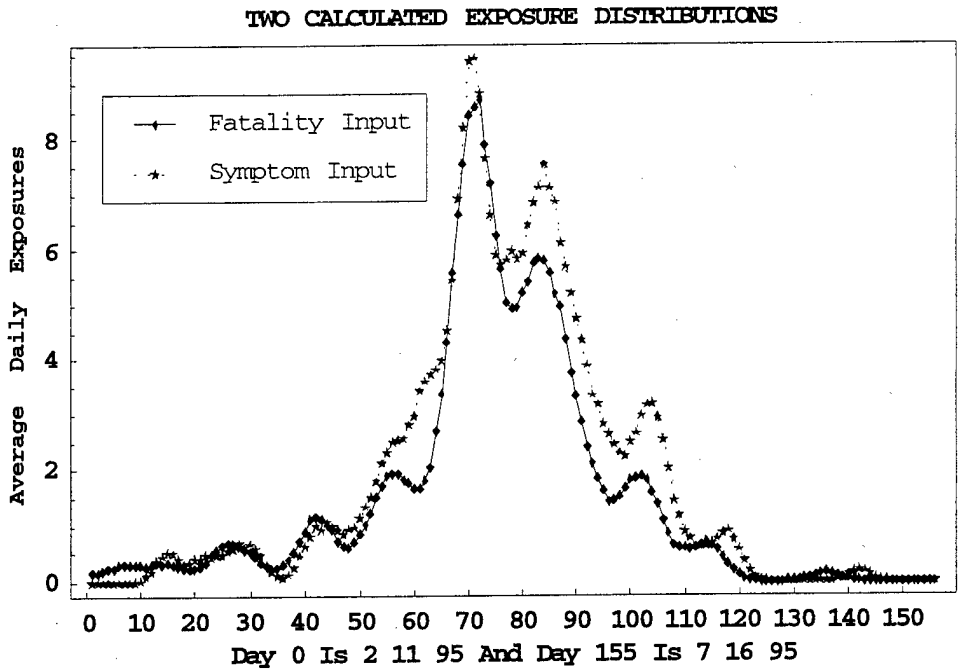

Figure III-3. Average Daily Exposures (Average New Infections Per Unit Time) for the Two Epidemiological Data Sets of Figures II-1 and II-2, Normally Distributed Random Variables, and 1000 Monte Carlo Trials.

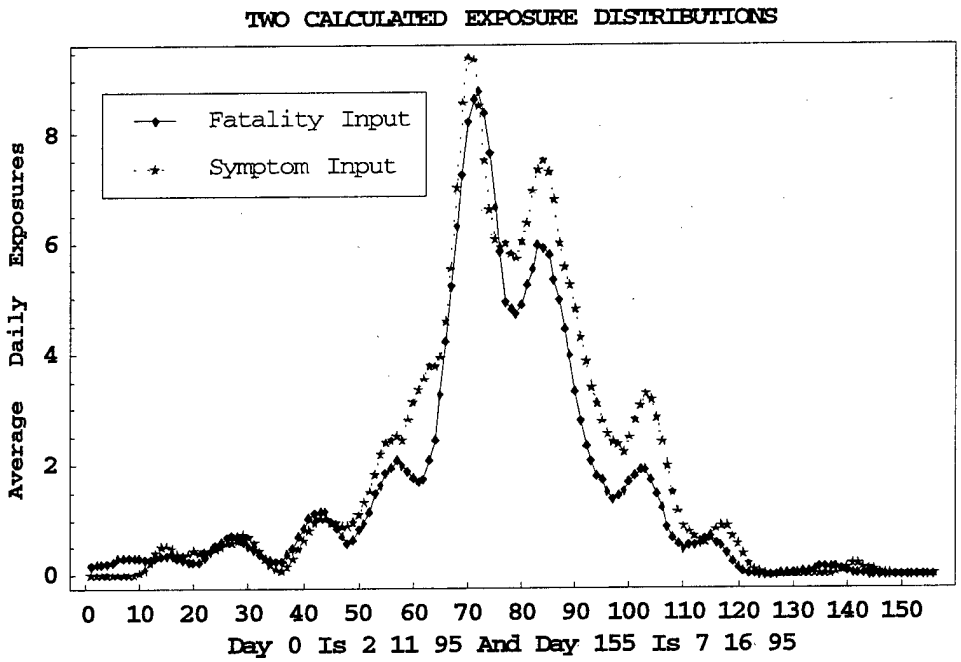

Figure III-4. Average Daily Exposures (Average New Infections Per Unit Time) for the Two Epidemiological Data Sets of Figures II-1 and II-2, Weibull and Lognormal Distributions, and 1000 Monte Carlo Trials.

Figure III-5 is a stacked bar chart that again displays average daily exposures for independent normal distributions. Red (or dark) bars in this chart represent the same temporal profile that appears in Figure III-3 for an input of fatality data. White bars signify average differences between symptom-related and fatality-related daily exposures, and these average differences are estimates of nonfatal new infections. Stacks of red and white bars in Figure III-5 thus make up a composite profile of average fatal and nonfatal daily exposures. Also, there are relatively few white bars with negative values in this profile and only two of these (at days 74 and 75) are appreciable.

Another stacked bar chart is displayed in Figure III-6, which is associated with the independent Weibull and lognormal distributions for σ and ζ. Red (or dark) bars therein comprise an alternative depiction of the profile in Figure III-4 that comes from fatality data, while the white bars again refer to nonfatal exposures (or new infections). Neither qualitative nor quantitative differences between Figures III-5 and III-6 are noteworthy. On the average, different distributional assumptions (normal-normal versus Weibull-lognormal distributions) lead to very similar composite exposures. One reason for this distributional insensitivity may be the fact that the Monte Carlo algorithm relies upon rounded (integer) values of the random variables.

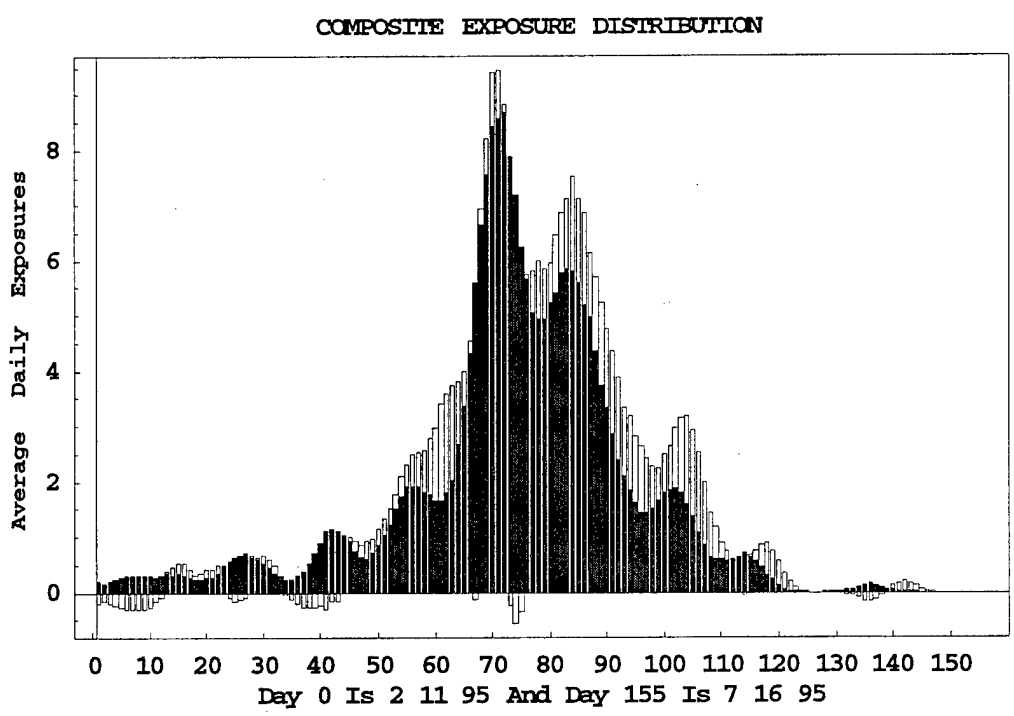

Figure III-5. Average Fatal (Red or Dark) and Nonfatal (White) Daily Exposures for the Two Epidemiological Data Sets of Figures II-1 and II-2, Normally Distributed Random Variables, and 1000 Monte Carlo Trials.

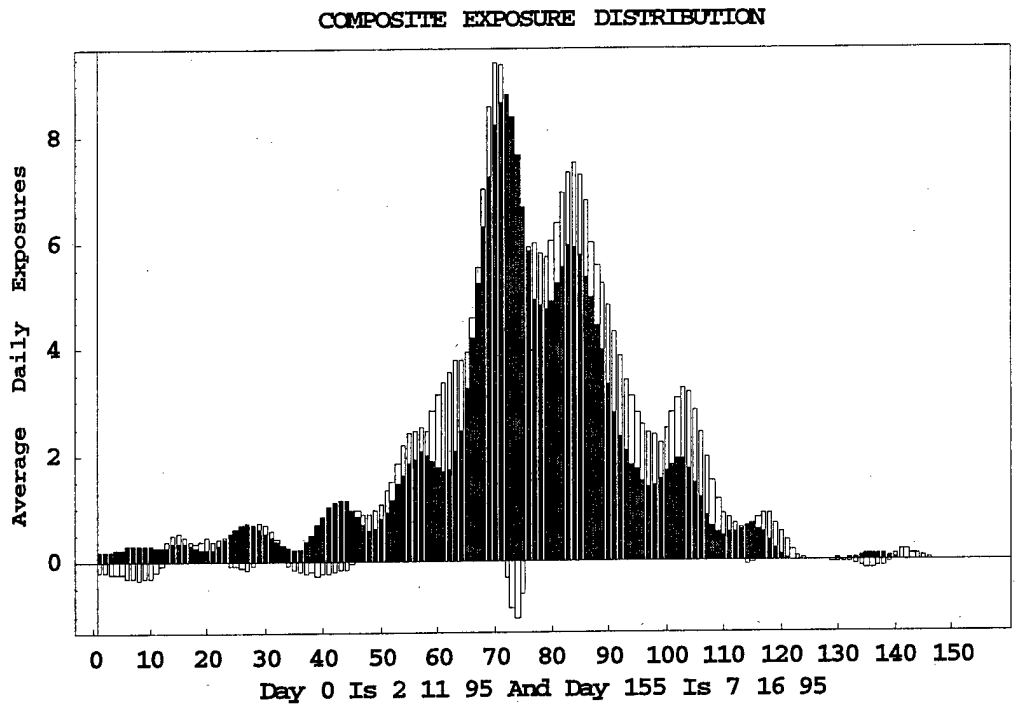

Figure III-6. Average Fatal (Red or Dark) and Nonfatal (White) Daily Exposures for the Two Epidemiological Data Sets of Figures II-1 and II-2, Weibull and Lognormal Distributions, and 1000 Monte Carlo Trials.

C. Average Daily New Infections in a Format for SEIR Calculations

Because the Haydon-Woolhouse-Kitching SEIR algorithm invokes the mean field assumption, the first incubation period should begin on day 0 and extend through day 8. Accordingly, there ought not to be any infectious individuals until day 9, and secondary infections shouldn't occur before day 10. The upshot is that average daily exposures in Figure III-5 or III-6 must be censored to reflect these initial conditions.

Negative average nonfatal exposures in Figures III-5 and III-6 pose another censoring problem and, in subsequent SEIR calculations, they will be ignored in favor of positive average fatal exposures. But when average nonfatal and fatal exposures are both positive quantities, their sum will be adopted as the censored value.

Figure III-7 demonstrates how the above censoring procedure alters Figure III-5. The arrow in Figure III-7 identifies the date (May 12, 1995, or day 90) when the international public health community became actively involved in the implementation of rigorous EHF controls.

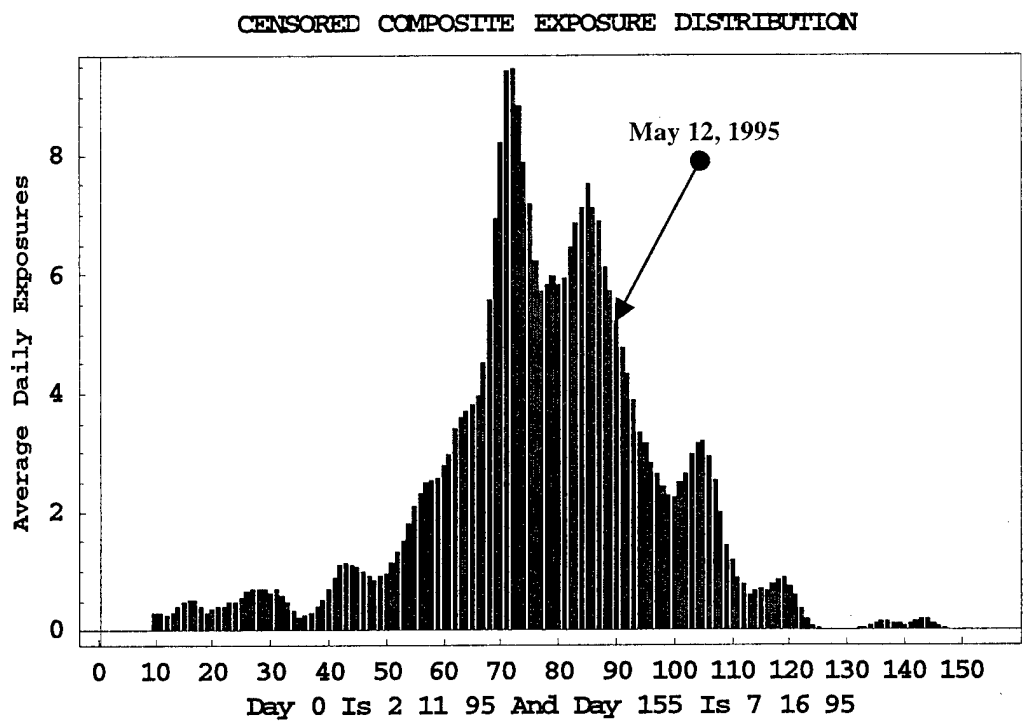

Figure III-7. Censored Version of Average Fatal and Nonfatal Daily Exposures in Figure III-5.

IV. SEIR RESULTS

A. Retrospective Investigation

The SEIR framework and Monte Carlo calculations of average new infections per day facilitate a better understanding of EHF dynamics in the 1995 Kikwit outbreak. There are several ways to numerically solve equations (1) through (6). Here, a rearrangement of equation (6) replaces the recursion relationship in equation (3), viz.,

(8) $I[n] = N_0 - S[n] - E[n] - R[n]$.

The numerical scheme thus evaluates S, E, I and R at each time step by utilizing known values of the function P in equations (1), (2), (8) and (4); subsequently, equation (5) enables an evaluation of the disease transmission rate, ξ.

Initial conditions for this investigation are as follows:

(9) $S[0] = N_0 - E[0]$,

(10) $E[0] = 1$,

and

(11) $I[0] = R[0] = 0.$

To fully account for the initial chain of events in the SEIR framework, two other conditions are essential. The first infected individual leaves the exposed cohort after the average incubation period (σa), and the same individual enters the removed cohort in accordance with the average infection-to-removal time (ζa). Mathematical statements[27] of these conditions are

(12) $E[\sigma_a] = E[\sigma_a - 1] + (P[\sigma_a - 1] - E[0])\times\Delta t$

and

(13) $R[\zeta_a] = 1.$

Some investigators argue for a "true mass-action assumption" and a disease transmission rate, β, that does not explicitly depend on the overall size of the time-independent total population, N_0.[28] Their SEIR model is almost identical to the one under consideration up to now, except that

(14) $\xi = \beta / N_0$

and, substituting for ξ in equation (5),

(15) $P[n]\times\Delta t / I[n] = \beta[n]\times S[n] / N_0.$

In the case of a limited outbreak within a large total population, the ratio of S to N_0 is always close to unity. This observation and equation (15) thus implies that $\beta[n]$ approaches the average number of new infections at time step n+1 per infectious individual at time step n.

The time-independent total population is basically an upper bound on the number of individuals who could be directly or indirectly contacted by members of the infectious cohort. For the 1995 EHF outbreak, a reasonable estimate of N_0 is Kikwit's total population of 200,000. The precise value of N_0 does not affect cohort temporal behavior

[27] A few comments about equations (12) and (13) are appropriate. The function P is assumed to be zero for negative arguments. That is, equation (2) simply cannot accommodate a movement out of the exposed cohort until one day after the average incubation period. Equation (12) guarantees that the initially infected individual will move out of the exposed cohort at the right time. It is also apparent that equation (4) can't allow an entry into the removed cohort until one day after the average infection-to-removal time. Hence, equation (13) assures that the initially infected individual will enter the removed cohort on time. And lastly, note the average incubation period (9 days) and the average infection-to-removal time (19 days) are as before.

[28] *Epidemic Models: Their Structure and Relation to Data, pp. 84-94.*

(unless everyone becomes infected); however, it can influence the disease transmission rate (especially ξ).

The calculated temporal profile for the removed cohort is in Figure IV-1, and the calculated final number of removals is 297 (237 deaths plus 60 recoveries). An incomplete reconciliation of fatal and nonfatal average daily exposures accounts for the difference between 297 removals and the original 291 cases of symptom onset.

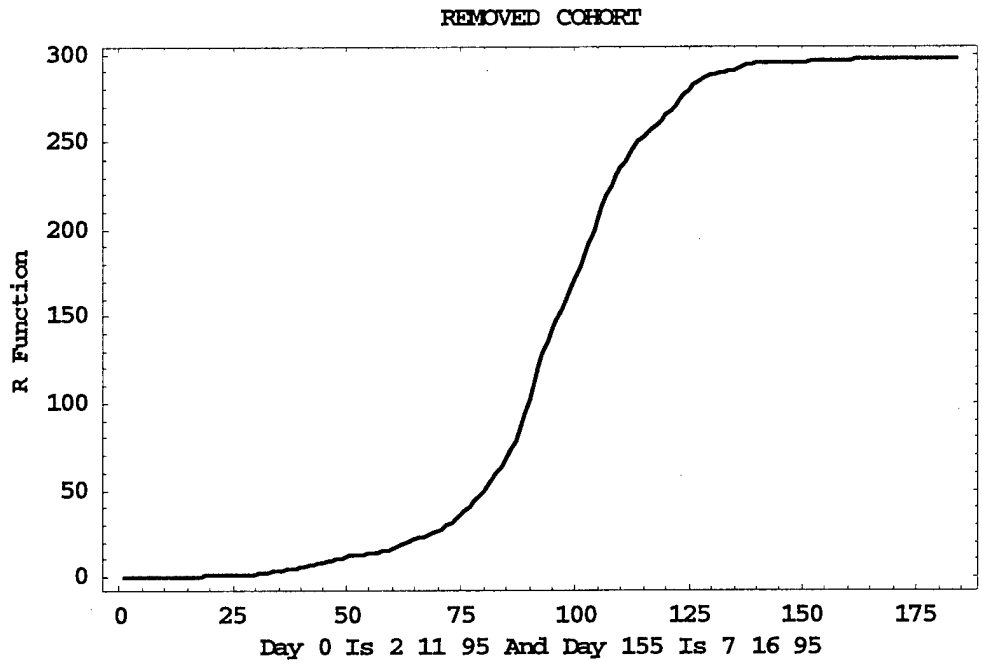

Figure IV-1. Time-Varying Total Number of Removed Individuals that Is Calculated from the Average Daily Exposures in Figure III-7.

Exposed and infectious cohort calculations are in Figure IV-2. The time history of the exposed cohort reaches its maximum on day 76, and the time history of the infectious cohort attains its somewhat larger maximum on day 86. In view of the fact that the average infectious period is one day longer than the average incubation period, it is not surprising that the infectious cohort can contain slightly more individuals than can the exposed cohort.

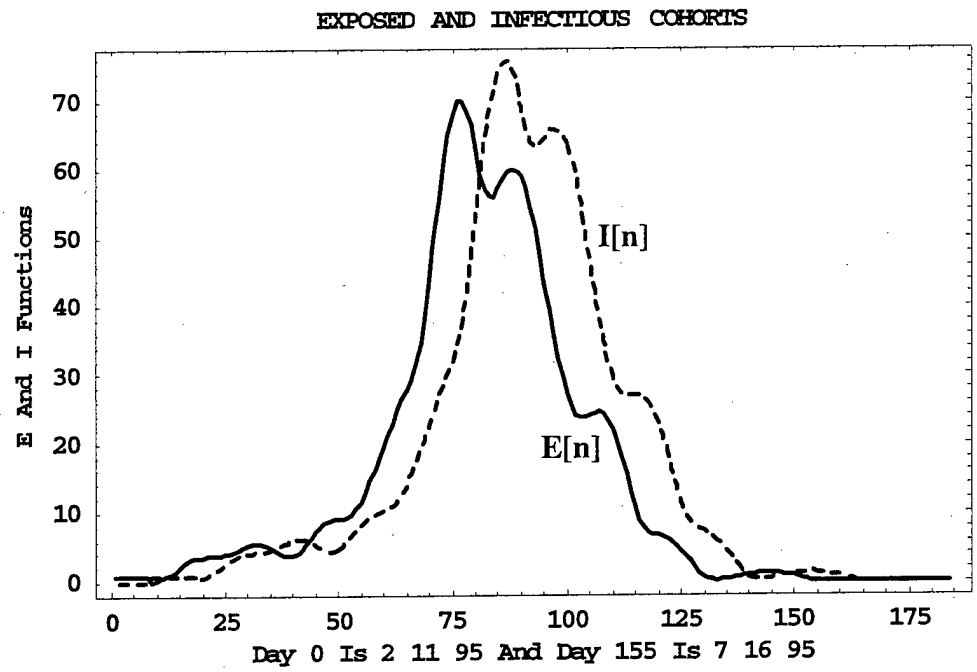

Figure IV-2. Instantaneous Numbers of Exposed (Incubating) and Infectious Individuals that Are Calculated from the Average Daily Exposures in Figure III-7.

Average daily exposures and temporal profiles for the susceptible and infectious cohorts control the temporal behavior of the disease transmission rate via equation (5).[29] Before discussing disease transmission numerical results, a brief review of the basic reproductive ratio (say, R_0) is useful.[30] If the average infectious period is υ_a, and if ξ_0 and β_0 are disease transmission rate constants, the formula for the basic reproductive ratio is

(16) $R_0 = \xi_0 \times N_0 \times \nu_a = \beta_0 \times \nu_a$.

Equation (16) defines R_0 as the average number of infections that are caused by a single infectious individual during his or her infectious period. A basic reproductive ratio of at least unity is therefore required to sustain an epidemic. Furthermore, this last observation and equation (16) yield the minimum epidemic-sustaining value of ξ_0 or β_0.

Figure IV-3 displays calculations of β for two sizes of the total population as well as the minimum constant value of β (i.e., β_0) that would have sustained the EHF epidemic. The impact of this total population variation can be explained by means of

[29] Of course, no transmission of any disease can occur whenever the infectious or susceptible cohort is empty.

[30] *Epidemic Models: Their Structure and Relation to Data*, pp. 17-33.

equation (15). For two identical outbreaks in large and small total populations, there can be no outbreak-to-outbreak differences either in the function P or in any of the SEIR cohorts. The logical inference is that different values of N_0 must alter the ratio of S to N_0, and that an offsetting change in β becomes a necessity. As an outbreak unfolds in a small total population, the ratio of S to N_0 decreases significantly over time but, during the same outbreak in a large total population, this ratio remains close to unity. Hence, an outbreak in a small total population generates a higher rate of disease transmission than does the identical outbreak in a large total population.

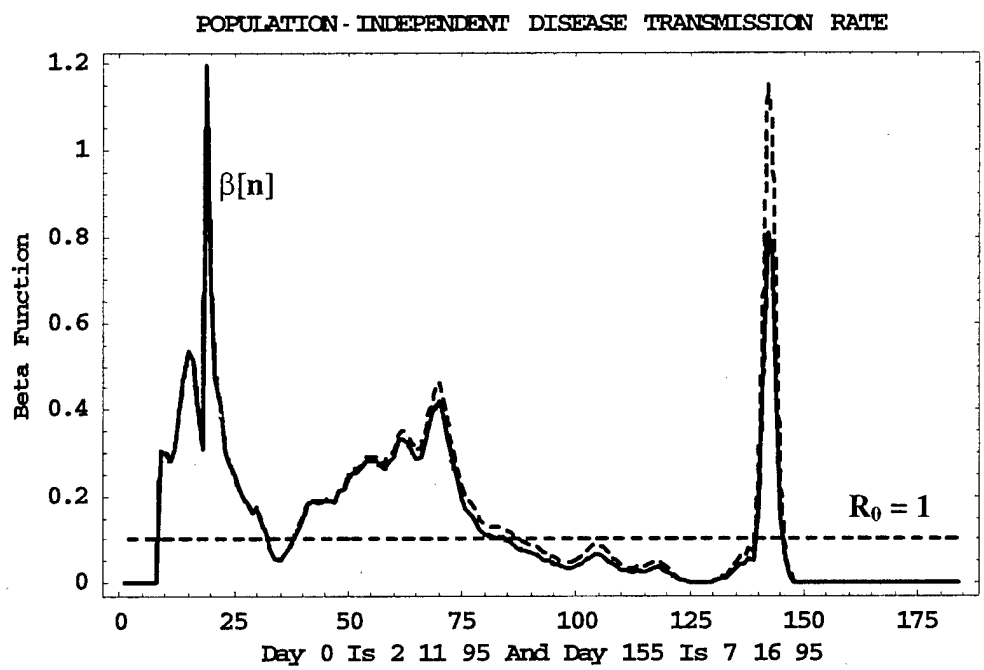

Figure IV-3. Calculated Time-Varying Rate of Disease Transmission, β, for the 1995 EHF Outbreak in Kikwit, DRC. The Solid (or Dashed) Curve Represents the Disease Transmission Rate for a Total Exposable Population of 200,000 (or 1,000).

Another feature of Figure IV-3 warrants some discussion, namely, the large spike within the timeframe from day 139 to day 148. Firstly, the last two fatalities in Figure II-1 are separated by 20 days, and the last two cases of symptom onset in Figure II-2 are separated by 22 days. Secondly, the last case of symptom onset precedes the last fatality by only four days. In terms of our SEIR model and its average parameter values, the last case of symptom onset and the last fatality comprise a "follow-on" outbreak, which is distinct from the "main" outbreak. This distinction surfaces in Figure III-7, and the transmission rate spike for the follow-on outbreak is likewise consistent with the calculated infectious cohort in Figure IV-2.

Lastly, the solid curve in Figure IV-3 is actually the superposition of two calculations for the total population of 200,000. The disease transmission rate β is one of the calculated quantities, as discussed above. The other calculated quantity is the left-hand side of equation (15), i.e., the average number of new infections at time step n+1 per infectious individual at time step n. Because the total population of 200,000 is much greater than the 300 or so removals, the two calculated quantities are indistinguishable.

B. Predictions for Equivalent Epidemiological Circumstances

The disease transmission rate in Figure IV-3 is a quantitative characterization of the epidemiological circumstances that surrounded the Kikwit EHF outbreak. Assuming equivalent circumstances will prevail throughout a future EHF epidemic, this transmission rate and a new set of initial conditions set the stage for a prediction. The numerical scheme for a prediction still relies on equations (1), (2), (4), (5) and (8). And since the function P is no longer a known quantity, it too must be evaluated in a stepwise fashion using known values of ξ or β and computed values of S and I.

The only change in the previous initial conditions is the replacement of equation (10) by

(17) $E[0] = 1, 5, 10, 15$ and 20.

Obviously, if the total exposable population is again 200,000, a "prediction" for one exposure or infection on day 0 should replicate cohort time histories in Figures IV-1 and IV-2.

In the foregoing retrospective analysis of the 1995 Kikwit outbreak, a large change in the total exposable population (from 200,000 to 1,000) did have an effect on the time history of β (particularly when the ratio of S to N_0 fell below 0.9 or so). This linkage between N_0 and β should be carefully considered in the predictive process. For the time being, input for cohort predictions is composed of a total population of 200,000, the appropriate time history of β in Figure IV-3, and equation (15). Comparable historical and future epidemiological circumstances suggest that even 20 initial infections are unlikely to produce more than about 6,000 (20×300) removals. And 6,000 removals would constitute only three percent of the total exposable population (or, necessarily, the final ratio of S to N_0 would be 0.97).

Exposed, infectious, and removed cohort time histories for the five different values of E[0] are in Figures IV-4, IV-5, and IV-6. For one initial infection, cohort time

histories in these figures do indeed match their counterparts in Figures IV-1 and IV-2. In the event of 20 initial exposures, predictions say that the exposed cohort could contain as many as 1,400 (20×70) individuals, that about 1,500 (20×75) individuals could be members of the infectious cohort, and that almost 6,000 removals would occur. This threefold observation, as well as an inspection of the five time histories for each cohort, point to linear behavior. As anticipated, the ratio of S to N_0 stays near unity and the function P really depends on only one cohort (I).

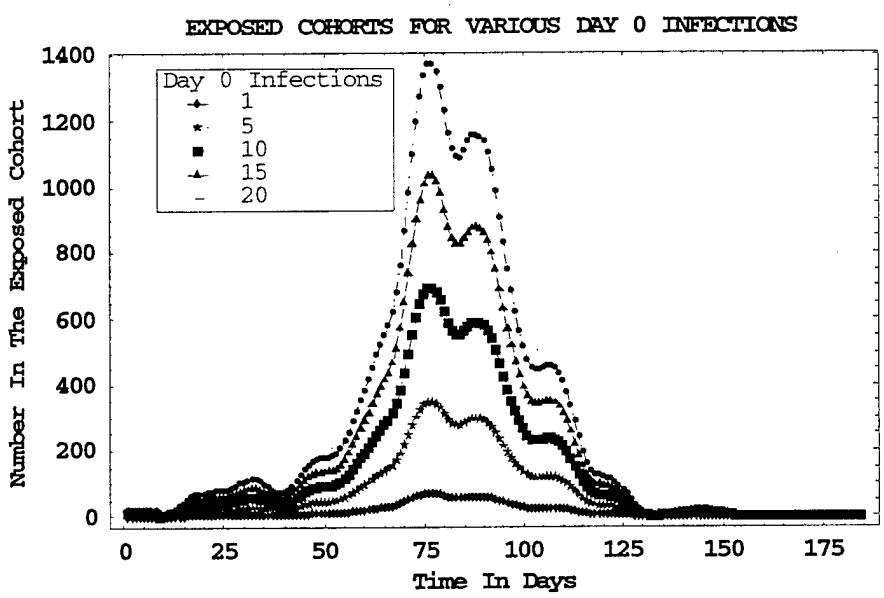

Figure IV-4. Instantaneous Number of Individuals in the Exposed Cohort for Different Initial Conditions (1, 5, 10, 15, and 20 Exposures on Day 0) and a Total Exposable Population of 200,000.

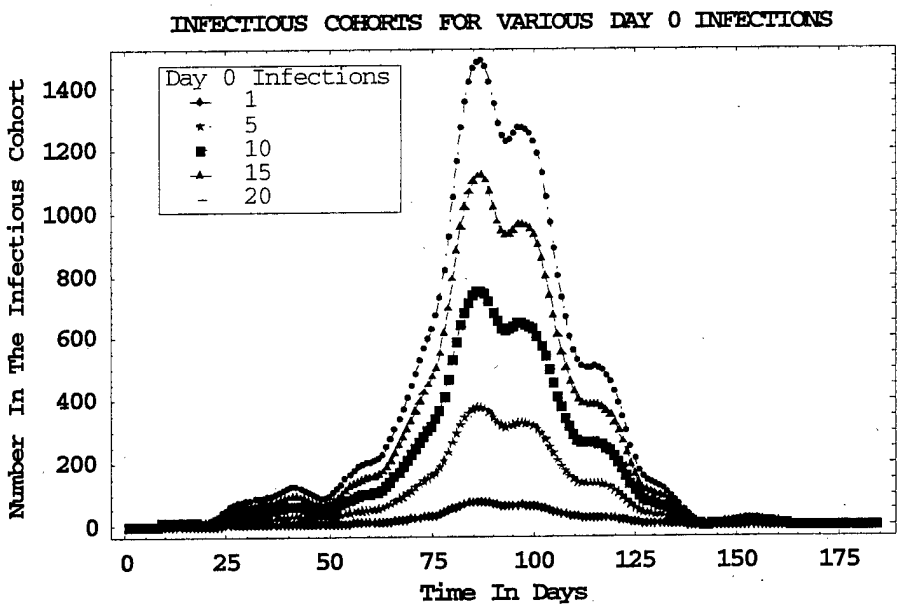

Figure IV-5. Instantaneous Number of Individuals in the Infectious Cohort for Different Initial Conditions (1, 5, 10, 15, and 20 Exposures on Day 0) and a Total Exposable Population of 200,000.

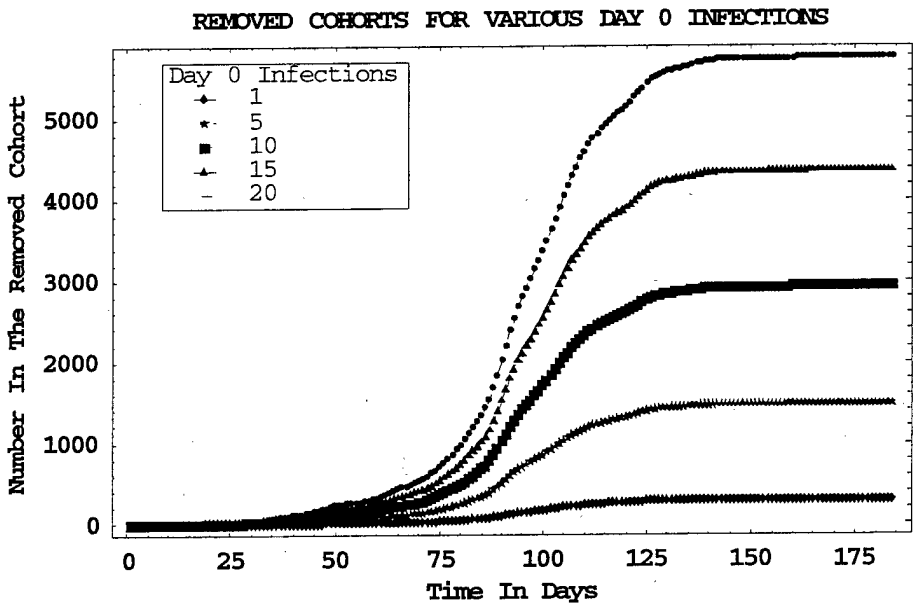

Figure IV-6. Cumulative Number of Individuals in the Removed Cohort for Different Initial Conditions (1, 5, 10, 15, and 20 Exposures on Day 0) and a Total Exposable Population of 200,000.

Figures IV-7, IV-8, and IV-9 display additional cohort predictions that are based on a total exposable population of 1,000 and the compatible β function. Unlike exposed cohort calculations in Figure IV-4, for instance, time histories in Figure IV-7 are not just temporal replicas of one another with scalable peak values. The onset of nonlinear cohort behavior occurs roughly at an elapsed time of 50 days, when the solid and dashed β curves diverge in Figure IV-3. Thereafter, in the presence of multiple initial infections, the decreasing ratio of S to N_0 (= 1,000) severely constrains the E, I, and R cohorts.

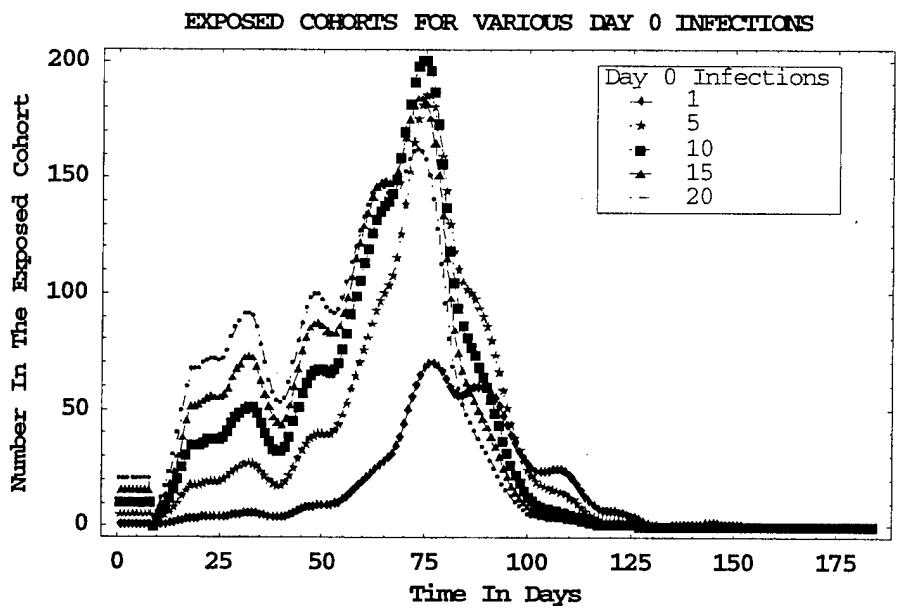

Figure IV-7. Instantaneous Number of Individuals in the Exposed Cohort for Different Initial Conditions (1, 5, 10, 15, and 20 Exposures on Day 0) and a Total Exposable Population of 1,000.

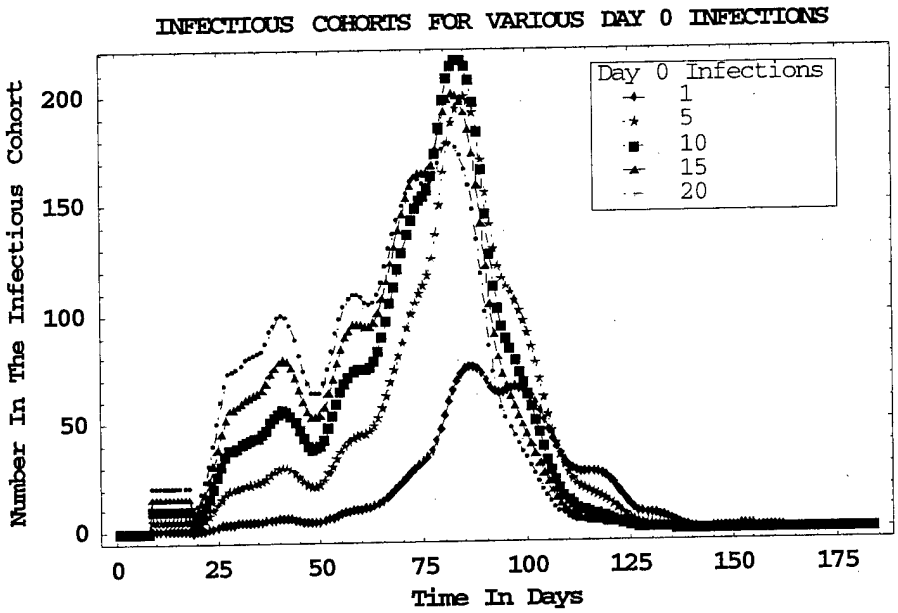

Figure IV-8. Instantaneous Number of Individuals in the Infectious Cohort for Different Initial Conditions (1, 5, 10, 15, and 20 Exposures on Day 0) and a Total Exposable Population of 1,000.

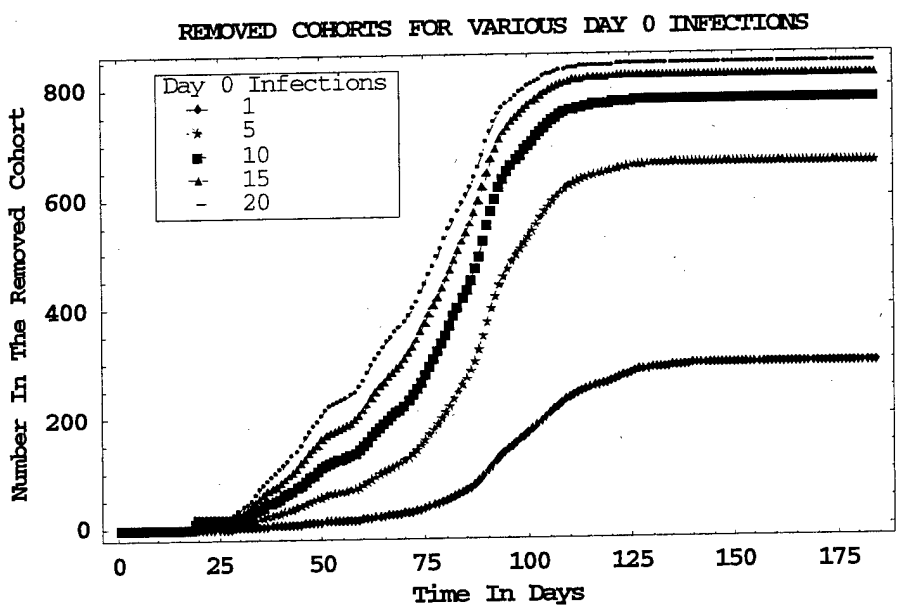

Figure IV-9. Cumulative Number of Individuals in the Removed Cohort for Different Initial Conditions (1, 5, 10, 15, and 20 Exposures on Day 0) and a Total Exposable Population of 1,000.

The total number of predicted removals is displayed in Figure IV-10 as a function of the initial infections, and the two curves in this figure portray removal predictions for total populations of 200,000 (solid curve) and 1,000 (dashed curve). Unconstrained and constrained removal predictions for 20 initial infections differ by a factor of 7, even though the variation in the exposable population is much greater (a factor of 200). This range of possible outcomes is in conformance with epidemiological circumstances of the 1995 Kikwit outbreak. To be sure, other epidemiological circumstances and another population variation could engender either a broader or a narrower predictive range.

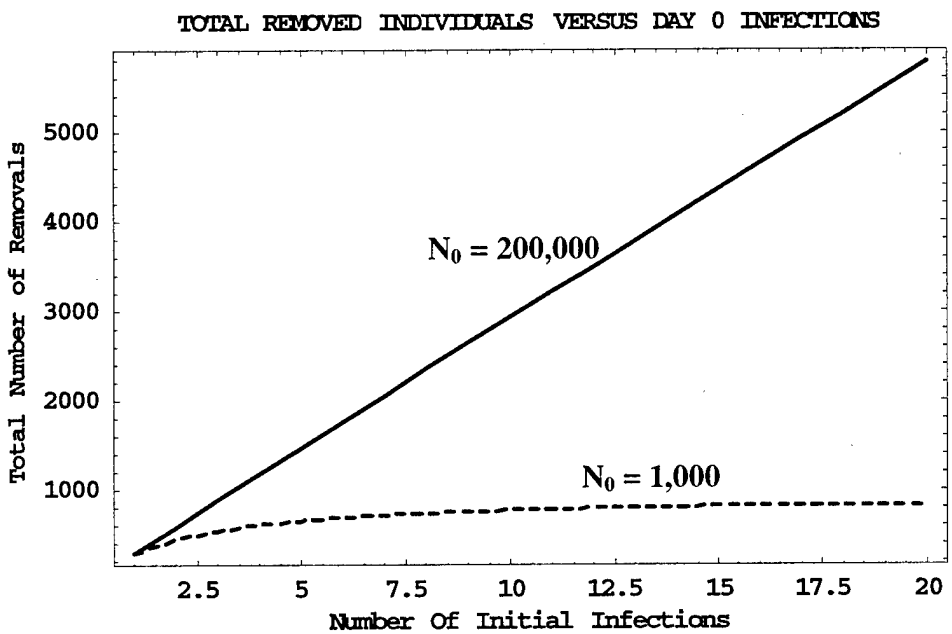

Figure IV-10. Total Number of Removals as a Function of the Number of Initial Infections for Exposable Populations of 200,000 and 1,000.

C. Unique Epidemiological Circumstances and Their Impact

An act of bioterrorism in a metropolitan area of the United States undoubtedly would involve unique epidemiological circumstances. Some of these circumstances may inhibit the spread of a contagious disease, but other circumstances might facilitate disease transmission. In the former category are prevailing U.S. medical capabilities, which are among the best in the world. Once numerous cases of symptom onset became known to U.S. health care providers and officials, the medical system's response would probably be prompt and effective. But the high mobility of people in and around large U.S. cities

would tend to rapidly transmit a contagious disease before the medical system could swing into action.

If a bioterrorist attack went undetected in a city, and if it infected hundreds or even thousands of individuals with the Ebola virus, people would experience EHF symptoms from 4 to 16 days after the attack. Most cases would not be apparent until day 10, and another week or more could be required to identify the disease and to understand the full extent of this bioterrorism event. Eventually, all face-to-face and physical contacts of every symptomatic individual would have to be traced and followed (or, perhaps, isolated) long enough to assure the absence of disease.

Unfortunately, an EHF vaccine does not exist and there are no effective drugs for either post-exposure prophylaxis or therapy. Today's medical systems can provide EHF patients with life support and/or compassionate care, but current medical capabilities are insufficient to abort or ameliorate the disease's natural course. Patient isolation, barrier nursing techniques, and strict disinfection procedures for biohazardous materials (including corpses) are primary EHF epidemic controls.[31]

Historical EHF outbreaks such as the one in Kikwit emphasize the importance of disease awareness and the avoidance of early medical mistakes. An optimistic view is that the U.S. medical system in a metropolitan area would respond to, for instance, 1,000 index cases with a high level of disease awareness and with little amplification of the disease in medical facilities. From a pessimistic perspective, however, most EHF cases in the U.S. would be managed with Kikwit-like levels of disease awareness and nosocomial disease transmission.

A thousand index cases and the attendant secondary infections could conceivably exhaust even the plentiful medical resources of a modern metropolis such as greater Washington, DC (with its population of 4,000,000). Under the pessimistic premise that Kikwit-like epidemiological circumstances would surround a future bioterrorism event in Washington, the time-varying rate of disease transmission in Figure IV-3 (solid curve) is applicable. And since a total of 300,000 (300×1,000) removals is still rather small with respect to an exposable population of 4,000,000, this number (300,000) of EHF cases is a plausible upper bound. Similarly, to bound cohort temporal behavior for 1,000 index cases, 50 should multiply cohort time histories in Figures IV-4, IV-5, and IV-6 for 20 initial infections.

---

[31] World Health Organization, *WHO Recommended Guidelines for Epidemic Preparedness and Response: Ebola Hemorrhagic Fever (EHF)*, WHO/EMC/DIS/97.7, July 1997, p.3.

The previous rough upper bounds are not in conflict with more precise numerical results in Figures IV-11, IV-12, IV-13, and IV-14. That is to say, for a total population of 4,000,000, these figures display cohort time histories with the following maximum values: 276,000 removals (Figures IV-13 and IV-14), 73,000 symptomatic cases (Figure IV-12), and 68,000 incubational cases (Figure IV-11).

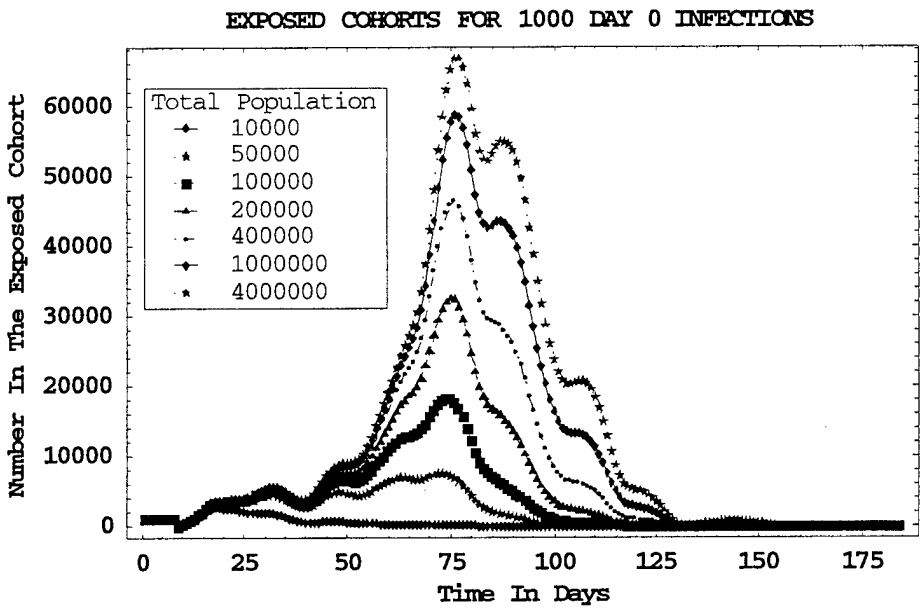

Figure IV-11. Instantaneous Number of Individuals in the Exposed Cohort for 1,000 Initial Infections and for Various Total Populations.

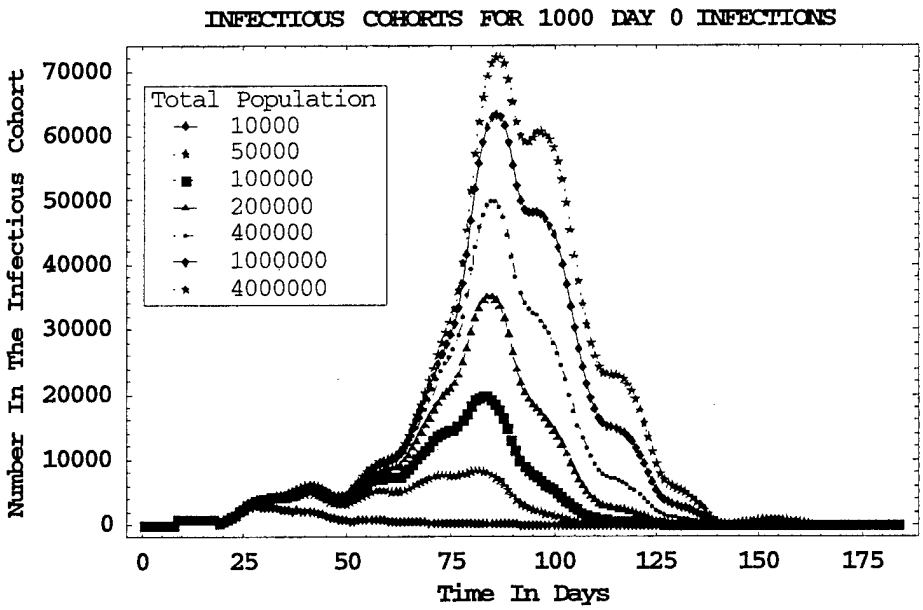

Figure IV-12. Instantaneous Number of Individuals in the Infectious Cohort for 1,000 Initial Infections and for Various Total Populations.

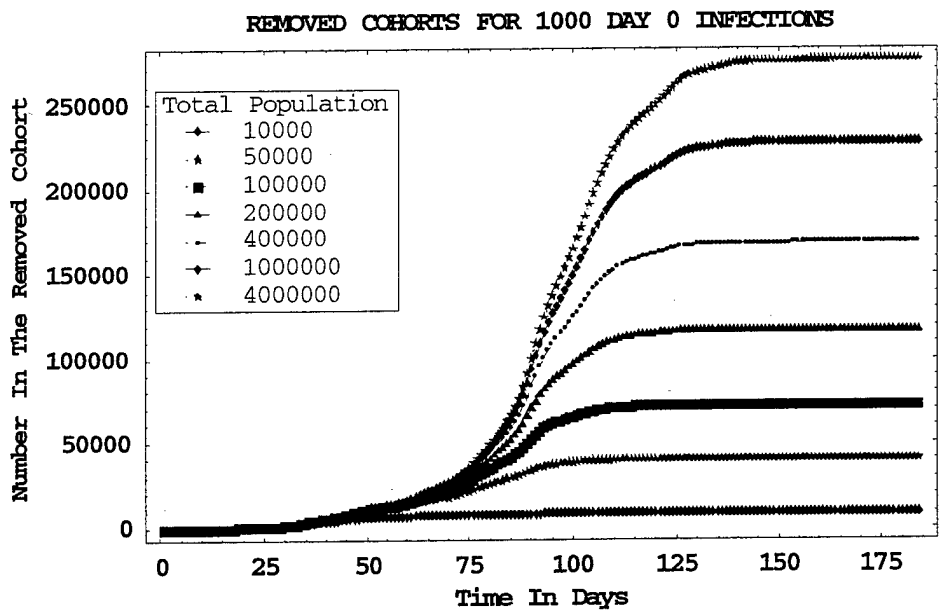

Figure IV-13. Cumulative Number of Individuals in the Removed Cohort for 1,000 Initial Infections and for Various Total Populations.

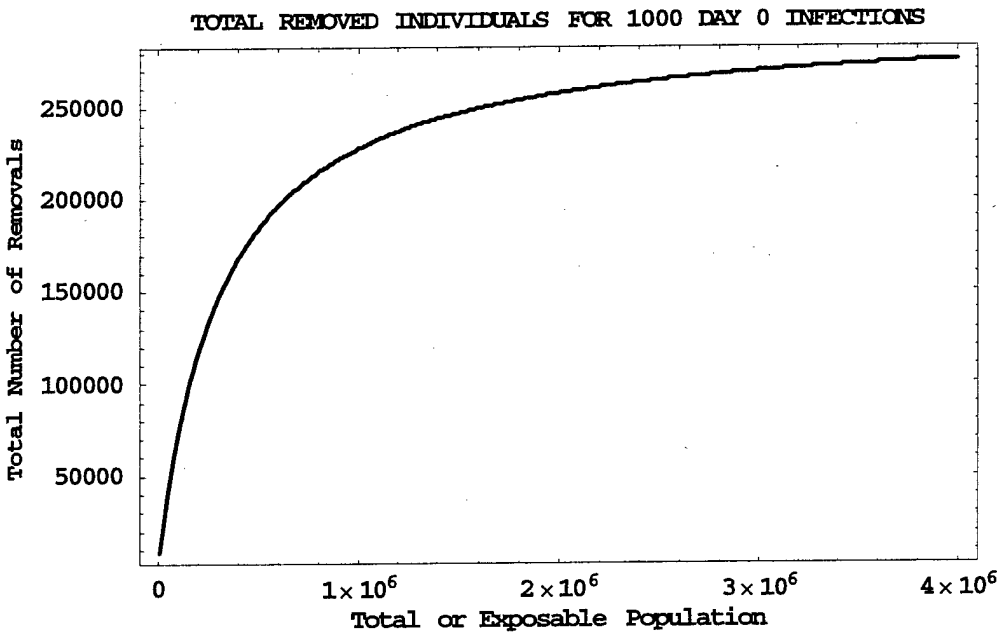

Figure IV-14. Total Number of Removals versus the Total Population for 1,000 Initial Infections.

Realistic lower-bound predictions of secondary EHF infections should reflect the implementation of stringent epidemic controls throughout the geographical area(s) of concern. According to Figure III-7, a considerable majority of Kikwit EHF infections happened before the emplacement of controls (day 90). The same figure illustrates that post-control average daily infections almost vanished within a period of 35 days (from day 90 to day 125). Figure IV-15 is the summation of Figures IV-11, IV-12, and IV-13. Each of its temporal profiles presents the overall time-varying number of exposed, infectious, and removed individuals for a specific total population. At any given time, therefore, a temporal profile in Figure IV-15 identifies how many removals would ultimately take place in the absence of any other new infections.

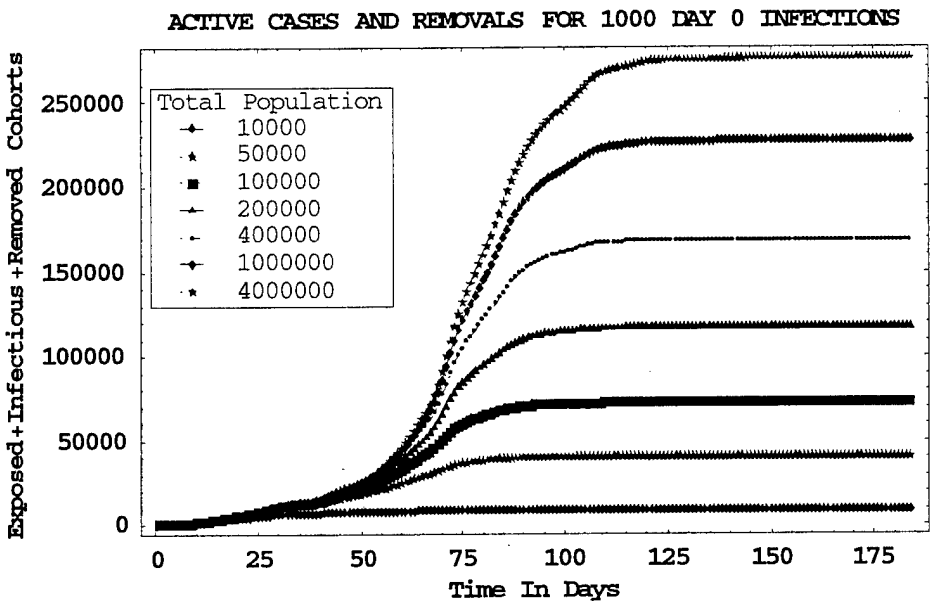

Figure IV-15. Instantaneous Projected Number of Removals for 1,000 Initial Infections and for Various Total Populations.

As recognized previously, the mobility of Washingtonians is likely to facilitate contacts with contagious people and, thereby, to accelerate disease transmission. Just as notable are the speed and reach of modern communication capabilities; i.e., the careful utilization of these capabilities might enable the U.S. medical system to swiftly and fully institute epidemic controls throughout the affected region(s). In the hypothetical situation where epidemic controls are emplaced on day 70 and completely effective on day 71 (as well as thereafter), Figure IV-15 says that 91,000 removals (80 percent deaths and 20 percent recoveries) should be anticipated under early Kikwit-like epidemiological

circumstances. Of course, the full realization of these 91,000 removals happens on day 89 (day 70 + 18 + 1) in Figure IV-13.

No attempt is made here to review the U.S. medical system and its epidemic response time following an undetected bioterrorist attack. Nevertheless, this author argues that pertinent historical outbreak data and some knowledge of potential response times are adequate to derive meaningful quantitative bounds on bioterrorism casualties. A parallel argument applies to a military theater of operations and U.S. military casualties due to biological warfare.

V. CONCLUDING OBSERVATIONS

Figures IV-1 through IV-15 typify what can be readily learned about the dynamics of a contagious disease and how to use this knowledge for predictive purposes. Predictions of BW and bioterrorism casualties inform military and public health care planners regarding dimensions of "unthinkable" medical crises. This paper advocates a semi-empirical predictive approach so those health care planners can relate BW and bioterrorism medical requirements to actual historical events. Arguably, semi-empirical casualty predictions are least likely to be either gross underestimates or unreal overestimates.

The role of epidemiological circumstances in the dynamics of a contagious disease is most important. As a case in point, consider the 1996 EHF outbreak in Mayibout 2, Gabon. Eighteen people found a chimpanzee cadaver in February and they proceeded to skin, butcher, cook, and eat the meat.[32] Because of another Gabon outbreak in late 1994 and early 1995, Gabonese medical personnel were well aware of EHF and ready to deal with it when advanced cases showed up at the same hospital (Makokou General) in early 1996. These medical personnel had the requisite equipment and materiel for barrier nursing techniques and, on the second day of the epidemic, they imposed rigorous infection controls.[33] Another significant factor is that the small Gabonese village of Mayibout 2 is remote and it takes a boat trip of six or seven hours to reach a larger population center. The outcome of this 1996 outbreak in Gabon was a total

[32] Alain-Jean Georges, Eric M. Leroy, Andre A. Renaut et al, *Ebola Hemorrhagic Fever Outbreaks in Gabon, 1994-1997: Epidemiologic and Health Control Issues*, JID, Vol. 179(Supplement 1), pp. S65-S75.

[33] None of the Gabonese medical people became infected with the Ebola virus during this outbreak.

of 31 fatal and nonfatal EHF cases, a far cry from the 315 cases in the 1995 DRC outbreak.

EHF outbreaks of the last 25 years clearly demonstrate that a) missteps in health care facilities can quickly transform one case of a contagious disease into a medical nightmare, and b) informed medical personnel and the right preparations can avert a disaster. Above and beyond the early identification of EHF cases and medical preparedness, a deeper understanding of EHF dynamics might reveal other opportunities to mitigate or interrupt an outbreak.

Semi-empirical predictions of BW and bioterrorism casualties for other contagious diseases will necessarily depend on historical outbreaks and associated epidemiological circumstances. Unfortunately, for diseases like pneumonic plague and glanders, usable and relevant epidemiological data may not exist. The epidemiological concept of a surrogate or substitute disease could prove to be a viable way to fill data gaps, but the development of such a concept is the subject of another study.

REPORT DOCUMENTATION PAGE

Form Approved
OMB No. 0704-0188

Public reporting burden for this collection of information is estimated to average 1 hour per response, including the time for reviewing instructions, searching existing data sources, gathering and maintaining the data needed, and completing and reviewing the collection of information. Send comments regarding this burden estimate or any other aspect of this collection of information, including suggestions for reducing this burden, to Washington Headquarters Services, Directorate for Information Operations and Reports, 1215 Jefferson Davis Highway, Suite 1204, Arlington, VA 22202-4302, and to the Office of Management and Budget, Paperwork Reduction Project (0704-0188), Washington, DC 20503.

1. AGENCY USE ONLY (Leave blank)	2. REPORT DATE February 2000	3. REPORT TYPE AND DATES COVERED Contributing Analysis

4. TITLE AND SUBTITLE Contagious Disease Dynamics for Biological Warfare and Bioterrorism Casualty Assessments	5. FUNDING NUMBERS DASW01-98 C 0067 DM-6-1845
6. AUTHOR(S) John N. Bombardt, Jr.	
7. PERFORMING ORGANIZATION NAME(S) AND ADDRESS(ES) Institute for Defense Analyses 1801 N. Beauregard Street Alexandria, VA 22311	8. PERFORMING ORGANIZATION REPORT NUMBER IDA Paper P-3488
9. SPONSORING/MONITORING AGENCY NAME(S) AND ADDRESS(ES) Joint Program Office for Biological Defense Falls Church, VA 22041	10. SPONSORING/MONITORING AGENCY REPORT NUMBER
11. SUPPLEMENTARY NOTES	
12a. DISTRIBUTION/AVAILABILITY STATEMENT Approved for public release; distribution unlimited.	12b. DISTRIBUTION CODE

13. ABSTRACT (Maximum 200 words)

This investigation focuses on the spread of a contagious disease subsequent to the military employment of a biological weapon or an act of bioterrorism. Of particular interest are expected or average time histories of four cohorts: (1) Susceptible individuals; (2) Exposed and infected (incubating) individuals; (3) Infectious (contagious) individuals and (4) Removed (noncontagious, alive, or dead) individuals. The objective SEIR curves characterize health care and mortuary service needs as functions of time for a known disease, for given initial conditions, and for an average time-varying rate of disease transmission. Such a disease transmission rate is a key predictive tool, and it is obtainable from a Monte Carlo analysis of historical outbreak data. Recently published epidemiological data for the 1995 Ebola hemorrhagic fever outbreak in Kikwit, Democratic Republic of the Congo, serves as an excellent vehicle to demonstrate the overall semi-empirical SEIR model.

14. SUBJECT TERMS Biological Warfare, Bioterrorism, Contagious Disease Dynamics, Disease Transmission Rate, Ebola Hemorrhagic Fever, Epidemiological Data, Monte Carlo Method, SEIR Epidemic Model, Semi-Empirical Casualty Predictions	15. NUMBER OF PAGES 186
	16. PRICE CODE

17. SECURITY CLASSIFICATION OF REPORT UNCLASSIFIED	18. SECURITY CLASSIFICATION OF THIS PAGE UNCLASSIFIED	19. SECURITY CLASSIFICATION OF ABSTRACT UNCLASSIFIED	20. LIMITATION OF ABSTRACT UL